Ligand Effects on the Blue Copper Site. Spectroscopic Studies of an Insulin-Stabilized Copper(II) Chromophore Incorporating an Exogenous Thiolate Ligand

Mark L. Brader,[†] Dan Borchardt,[‡] and Michael F. Dunn*,[†]

Contribution from the Departments of Biochemistry and Chemistry, University of California at Riverside, Riverside, California 92521. *Received October 16, 1991*

Abstract: Insulin-stabilized type 1 $Cu^{II}N_3L$ chromophores, in which L represents an exchangeable aromatic thiolate ligand, have been characterized by electron spin resonance (ESR), circular dicroism (CD), and UV-visible electronic absorption spectroscopy. The charge-transfer (CT) and ESR characteristics of these chromophores are strongly influenced by the nature of the thiolate ligand that coordinates to the copper. The complexes formed with pentafluorobenzenethiolate (PFBT) and tetrafluorobenzenethiolate (TFBT) possess axial ESR spectra ($g_\parallel = 2.065$, $g_\perp = 2.264$, $A_\parallel = 87 \times 10^{-4}$ cm^{-1}) that are analogous to those of the blue copper proteins plastocyanin and azurin. Furthermore, the resonance Raman spectrum of the PFBT complex is characterized by bands at 422, 393, 348, and 213 cm^{-1}, features which indicate a strong resemblance to the resonance Raman spectrum of azurin. The complexes formed with benzenethiolate (BT) and 4-methylbenzenethiolate (4-MeBT) possess ESR spectra ($g_x = 2.025$, $g_y = 2.090$, $g_z = 2.230$, $A_x = 60 \times 10^{-4}$ cm^{-1}, $A_y = 33 \times 10^{-4}$ cm^{-1}, $A_z = 38 \times 10^{-4}$ cm^{-1} and $g_x = 2.020$, $g_y = 2.090$, $g_z = 2.210$, $A_x = 60 \times 10^{-4}$ cm^{-1}, $A_y = 32 \times 10^{-4}$ cm^{-1}, $A_z = 42 \times 10^{-4}$ cm^{-1}, respectively) that display substantial rhombic character and unusual hyperfine couplings, features which are strikingly similar to those that distinguish the ESR spectrum of the structurally uncharacterized blue copper protein, stellacyanin. The ligand 2-pyridinethiolate (2-PT) forms a complex possessing type 2 ESR ($g_\parallel = 2.240$, $g_\perp = 2.060$, $A_\parallel = 152 \times 10^{-4}$ cm^{-1}) and optical ($\lambda_{max} = 500$ nm, $\epsilon_{max} = 230$ M^{-1} cm^{-1}; $\lambda_{max} = 720$ nm, $\epsilon_{max} = 250$ M^{-1} cm^{-1}) characteristics that are similar to those of the copper site in native bovine superoxide dismutase. This complex is proposed to incorporate 2-pyridinethiolate coordinated in a bidentate mode, thus forming a pentacoordinate Cu(II) center. Collectively, the ESR and CT data for the type 1 copper chromophores indicate that substitution in the aromatic ring of the coordinated benzenethiolate group affects the covalency of the Cu(II)-S interaction, resulting in perturbations of the Cu(II) site symmetry. It is concluded that an increased covalency of the Cu(II)-S(thiolate) bond in the pseudotetrahedral $Cu^{II}N_3S$ unit can induce a change in the ESR spectrum from axially symmetric to one that possesses stellacyanin-like rhombic ESR parameters.

Introduction

The exotic spectroscopic properties of blue (or type 1) copper proteins have stimulated considerable interest in the structural and electronic characteristics of the copper sites in these systems.[1] The blue copper spectral features comprise an unusually small ESR hyperfine coupling constant ($A_\parallel < 70 \times 10^{-4}$ cm^{-1}) and a very intense optical absorption envelope ($\epsilon_{(600-630)} = 3000-5000$ M^{-1} cm^{-1}) with which distinctive resonance Raman bands are associated. The origins of these features have been elucidated via single-crystal X-ray crystallographic studies[2] of several blue copper proteins in conjunction with detailed spectroscopic studies[3-9] of these proteins and relevant model systems.[10] The blue copper protein crystal structures all identify highly distorted copper sites that incorporate two histidine imidazolyl nitrogens, a cysteine thiolate sulfur, and a methionine thioether sulfur as ligands to the copper. One impetus for extending chemical experience of the type 1 copper center beyond this now familiar $Cu^{II}N_2$(His)-S(Cys)S(Met) structural motif stems from interest in atypical copper proteins, such as stellacyanin and cytochrome c oxidase, which possess exceptional spectroscopic properties but which remain structurally uncharacterized. Stellacyanin is a blue copper protein that contains a single type 1 copper center. The spectrochemical properties of stellacyanin[1d,11] are distinctive in comparison to the other blue copper proteins; notably, the ESR spectrum is decidedly rhombic and displays peculiar hyperfine splittings. Spectroscopic studies[12-14] indicate that two histidines and a cysteine residue ligate the copper; however, the copper site in stellacyanin cannot be entirely analogous to those of the structurally characterized blue copper proteins because stellacyanin does not contain methionine. The uncertainty regarding the stellacyanin active site exemplifies the difficulty associated with relating the spectroscopic nuances of pseudotetrahedral Cu(II) sites to specific elements of biological structure and function. This difficulty highlights the need for a type 1 model system which allows the relationship between structure and spectroscopic behavior to be probed by rational manipulation of the copper site.

* Author to whom correspondence should be addressed.
[†] Department of Biochemistry.
[‡] Department of Chemistry.

(1) For reviews, see: (a) Fee, J. A. *Struct. Bonding (Berlin)* **1975**, *23*, 1-60. (b) Gray, H. B.; Solomon, E. I. In *Copper Proteins*; Spiro, T. G., Ed.; Wiley: New York, 1981; Vol. 3, pp 1-39. (c) Solomon, E. I.; Penfield, K. W.; Wilcox, D. E. *Struct. Bonding (Berlin)* **1983**, *53*, 1-57. (d) Lappin, A. G In *Metal Ions in Biological Systems. Copper Proteins*; Sigel, H., Ed.; Marcel Dekker: New York, 1981; Vol. 13, pp 15-71. (e) Adman, E. T. In *Advances in Protein Chemistry. Copper Protein Structures*; Anfinsen, C. B., Edsall, J. T., Eisenberg, D., Richards, F. M., Eds.; Academic Press: New York, 1991; Vol. 42, pp 145-197.

(2) (a) Norris, G. E.; Anderson, B. F.; Baker, E. N. *J. Mol. Biol.* **1983**, *165*, 501-521. (b) Norris, G. E.; Anderson, B. F.; Baker, E. N. *J. Am. Chem. Soc.* **1986**, *108*, 2784-2785. (c) Baker, E. N. *J. Mol. Biol.* **1988**, *203*, 1071-1095. (d) Adman, E. T.; Jensen, L. H. *Isr. J. Chem.* **1981**, *21*, 8-12. (e) Korszun, Z. R. *J. Mol. Biol.* **1987**, *196*, 413-419. (f) Guss, J. M.; Freeman, H. C. *J. Mol. Biol.* **1983**, *169*, 521-563. (g) Adman, E. T.; Stenkamp, R. E.; Sieker, L. C.; Jensen, L. H. *J. Mol. Biol.* **1978**, *123*, 35-47. (h) Guss, J. M.; Merritt, E. A.; Phizackerley, R. P.; Hedman, B.; Murata, M.; Hodgson, K. O.; Freeman, H. C. *Science* **1988**, *241*, 806-811. (i) Adman, E. T.; Stewart, T.; Bramson, R.; Petratos, K.; Banner, D.; Tsernoglou, D.; Beppu, T.; Watanabe, H. *J. Biol. Chem.* **1989**, *264*, 87-99. (j) Messerschmidt, A.; Rossi, A.; Ladenstein, R.; Huber, R.; Bolognesi, M.; Gatti, G.; Marchesini, A.; Petruzelli, R.; Finazzi-Agro, A. *J. Mol. Biol.* **1989**, *206*, 513-529.

(3) Solomon, E. I.; Hare, J. W.; Dooley, D. M.; Dawson, J. H.; Stephens, P. J.; Gray, H. B. *J. Am. Chem. Soc.* **1980**, *102*, 168-178.

(4) Penfield, K. W.; Gay, R. R.; Himmelwright, R. S.; Eickman, N. C.; Norris, V. A.; Freeman, H. C.; Solomon, E. I. *J. Am. Chem. Soc.* **1981**, *103*, 4382-4388.

(5) Penfield, K. W.; Gewirth, A. A.; Solomon, E. I. *J. Am. Chem. Soc.* **1985**, *107*, 4519-4529.

(6) Dawson, J. H.; Dooley, D. M.; Clark, R.; Stephens, P. J.; Gray, H. B. *J. Am. Chem. Soc.* **1979**, *101*, 5046-5053.

(7) Gewirth, A. A.; Solomon, E. I. *J. Am. Chem. Soc.* **1988**, *110*, 3811-3819.

(8) Woodruff, W. H.; Norton, K. A. *J. Am. Chem. Soc.* **1983**, *105*, 657-658.

(9) Ainscough, E. W.; Bingham, A. G.; Brodie, A. M.; Ellis, W. R.; Gray, H. B.; Loehr, T. M.; Plowman, J. E.; Norris, G. E.; Baker, E. N. *Biochemistry* **1987**, *26*, 71-82.

(10) (a) Schugar, H. J. In *Copper Coordination Chemistry: Biochemical and Inorganic Perspectives*; Karlin, K., Zubieta, J., Eds.; Adenine Press: Guilderland, NY, 1983; pp 43-74. (b) Knapp, S.; Keenan, T. P.; Zhang, X.; Fikar, R.; Potenza, J. A.; Schugar, H. J. *J. Am. Chem. Soc.* **1990**, *112*, 3452-3464.

0002-7863/92/1514-4480$03.00/0

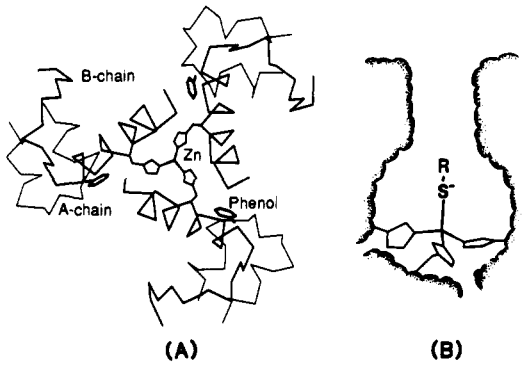

Figure 1. View down the 3-fold symmetry axis of one half of the Zn(II)-R_6 insulin hexamer showing the structural arrangement of the three subunits that form one zinc site (A). The locations of the protein-bound phenol molecules are shown also. Schematic representation of the copper environment postulated herein for the type 1 sites of the Cu(II)-R_6-thiolate complexes (B). The exogenous thiolate ligand is designated R-S^- and is constrained by an ~8-Å long cylindrical tunnel that is formed by the B chain helices. A pseudotetrahedral array about the copper is completed by three HisB10 imidazolyl nitrogens. Coordinates for these drawings were kindly provided by Guy G. Dodson (University of York), and the computer graphics for the drawings were performed by Ole Hvilsted Olsen (Novo Research Institute).

Unfortunately, attempts to develop synthetic model analogues of the type 1 copper site have met with notorious difficulty due to the redox instability of the Cu(II)–thiolate interaction[15] and the marked preference of the Cu(II) ion for tetragonal rather than pseudotetrahedral coordination geometries.

The Cu(II)-substituted R-state insulin hexamer[16-18] is one system that has been postulated to stabilize Cu(II)–thiolate ligation in a distorted tetrahedral $Cu^{II}N_3S$(thiolate) environment (Figure 1). X-ray crystallographic studies[19-22] of Zn(II)–insulin hexamers have identified a set of three structures designated[23] as T_6, T_3R_3, and R_6. The R_6 hexamer[21,22] is stabilized by six phenol molecules which bind to hydrophobic pockets formed between adjacent subunits. This structure incorporates two identical Zn sites, each with a distorted tetrahedral arrangement of three B10 histidines and one chloride[21] or phenolate ion[22] (Figure 1A). The M(II)-R_6[24] insulin hexamer provides, in effect, a constrained tridentate imidazolyl N_3 chelate in which a fourth coordination position is accessible to an exogenous ligand (Figure 1B). With copper–insulin, the spectrochemical versatility of this system is noteworthy because it permits the investigation of a type 1 Cu(II) site in which the thiolate ligand may be varied. In this report we have characterized spectroscopically several Cu(II)–R_6–thiolate adducts with the goal of demonstrating how perturbations of the Cu(II)–thiolate bond affect the spectral properties of the type 1 Cu(II) site.

Table I. Electronic Absorption Data[a] for the Cu(II)-R_6–Thiolate Complexes

thiolate[b]	
PFBT	372 (1250), 406 (1100), 626 (1700), 880[c] (520)
TFBT	369 (1200), 416 (1250), 630 (1800), 880[c] (550)
BT	310 (2700), 378 (900), 450 (700), 696 (2700), 890[c] (1700)
4-MeBT	315[d] (2300), 390 (700), 448 (530), 702 (2500), 890[c] (2200)
2-PT	500 (230), 720 (250)
4-PT	432 (1000), 646 (1250), 900[c] (400)

[a] λ_{max}, nm (ϵ_{max}, M^{-1} cm^{-1}). ϵ_{max} = observed extinction coefficient calculated with respect to metal ion concentration. [b] BT = benzenethiolate, PFBT = pentafluorobenzenethiolate, TFBT = tetrafluorobenzenethiolate, 4-MeBT = 4-methylbenzenethiolate, 2-PT = 2-pyridinethiolate, 4-PT = 4-pyridinethiolate. [c] Broad. [d] Shoulder.

Experimental Section

Preparation of the Insulin Complexes. Cu(II)-T_6 hexamer solutions were prepared by the stoichiometric addition of Cu^{2+} ions to solutions of metal-free human insulin in the ratio of two Cu^{2+} ions per six insulin subunits (M = 5800). These solutions were prepared in 50 mM Tris-ClO_4 buffer, pH 7.5. Insulin concentrations were determined from the absorbance at 280 nm ($\epsilon = 5.7 \times 10^3$ M^{-1} cm^{-1}). Except where indicated, the Cu(II)-R_6–thiolate complexes were obtained upon the addition of thiolate to the solution of Cu(II)-substituted insulin hexamer in the presence of 100 mM resorcinol.[25] Co(II)-R_6–thiolate solutions were prepared as described previously.[26]

A slow bleaching of the Cu(II)-R_6–thiolate complexes occurs at room temperature. This process proceeds at varying rates, depending upon the thiolate ligand. The ESR spectral signals of the Cu(II)-R_6–thiolate complexes were typically 50% less intense than that of the original Cu(II)-T_6 solution, indicating that an appreciable degree of reduction of Cu(I) had taken place. Reduction of Cu(II)-R_6–thiolate complexes has been shown to yield the corresponding optically- and ESR-unobservable Cu(I)-R_6–thiolate complexes.[17] Thus the extinction coefficients observed for the UV–visible spectra must be regarded as minimum values.

Electronic Absorption and Circular Dichroism Spectroscopy. Spectra were recorded at 298 K immediately following the preparation of the Cu(II)-R_6–thiolate complexes using a 1:1 M/thiolate ratio. Electronic absorption spectra were recorded using a Hewlett-Packard HP8450A spectrophotometer for the 300–800 nm range and a Cary 2390 spectrophotometer for the 800–1100 nm range. Circular dichroism spectra obtained using a JASCO J-600 spectropolarimeter are reported in the range 300–800 nm.

ESR Spectroscopy. X-band ESR spectra (9.21 GHz) were recorded on frozen (110 K) solutions in quartz tubes utilizing a Bruker ER200D ESR spectrometer equipped with a Hewlett-Packard 5350B microwave frequency counter and a Bruker ER035M gaussmeter. Spectra were recorded immediately following the preparation of the Cu(II)-R_6–thiolate complexes using a 1:2 M/thiolate ratio. No color changes due to freezing and thawing the solutions for ESR spectroscopy were observed.

ESR Simulations.[27] These were performed using the program QPOW.[28] The simulations utilized a spin Hamiltonian of the form given by eq 1

$$\mathcal{H} = \beta \mathbf{H}\cdot\mathbf{g}\cdot S + S\cdot\mathbf{A}\cdot I \qquad (1)$$

where H is the magnetic field vector, S and I are the electron and nuclear spins respectively, $\mathbf{g}$ is the g tensor, $\mathbf{A}$ is the hyperfine tensor, and β is the Bohr magneton. Transitions where $\Delta M_I \neq 0$ were not included in the simulations. A and g were assumed to have the same principal axes, and a Gaussian lineshape was used. The values of the g and A parameters giving the best agreement with the experimental data were found by trial and error.

Resonance Raman Spectroscopy. Spectra were recorded at 298 K on samples in glass melting point capillary tubes using a Dilor XY laser

(11) Malmstrom, B. G.; Reinhammar, B.; Vanngard, T. *Biochim. Biophys. Acta* **1970**, *205*, 48–57.
(12) Rist, G. H.; Hyde, J. S.; Vanngard, T. *Proc. Natl. Acad. Sci. U.S.A.* **1970**, *67*, 79–86.
(13) Mims, W. B.; Peisach, J. *Biochemistry* **1976**, *15*, 3863–3869.
(14) Roberts, J. E.; Brown, T. G.; Hoffman, B. M.; Peisach, J. *J. Am. Chem. Soc.* **1980**, *102*, 825–829.
(15) Anderson, O. P.; Perkins, C. M.; Brito, K. K. *Inorg. Chem.* **1983**, *22*, 1267–1273.
(16) Brader, M. L.; Dunn, M. F. *J. Am. Chem. Soc.* **1990**, *112*, 4585–4587.
(17) Brader, M. L.; Borchardt, D.; Dunn, M. F. *Biochemistry*, in press.
(18) Brader, M. L.; Dunn, M. F. *Trends Biochem. Sci.* **1991**, *16*, 341–345.
(19) Baker, E. N.; Blundell, T. L.; Cutfield, J. F.; Cutfield, S. M.; Dodson, E. J.; Dodson, G. G.; Crowfoot-Hodgkin, D. M.; Hubbard, R. E.; Isaacs, N. W.; Reynolds, C. D.; Sakabe, K.; Sakabe, N.; Vijayan, N. M. *Philos. Trans. R. Soc. London* **1988**, *319*, 369–456.
(20) Smith, G. D.; Swenson, D. C.; Dodson, E. J.; Dodson, G. G.; Reynolds, C. D. *Proc. Natl. Acad. Sci. U.S.A.* **1984**, *81*, 7093–7097.
(21) Derewenda, U.; Derewenda, Z.; Dodson, E. J.; Dodson, G. G.; Reynolds, C. D.; Smith, G. D.; Sparks, C.; Swenson, D. *Nature* **1989**, *338*, 594–596.
(22) Smith, G. D.; Dodson, G. G. *Biopolymers* **1992**, *32*, 441–445.
(23) Kaarsholm, N. C.; Ko, H.-C.; Dunn, M. F. *Biochemistry* **1989**, *28*, 4427–4435.
(24) M(II)-T_6 and M(II)-R_6 denote the metal-substituted T_6 and R_6 insulin hexamers, respectively, where M may be Cu, Co, or Zn. Two chemically equivalent metal ions are bound per hexamer.
(25) Our previous studies (ref 26 and Choi et al., unpublished results) have shown that a wide variety of phenolic derivatives stabilize the R_6 conformation of the M(II)-substituted insulin hexamer. For Co(II)- and Cu(II)–insulin hexamers, resorcinol displaces the $T_6 = R_6$ equilibrium more strongly in favor of the R_6 species than does phenol.
(26) Brader, M. L.; Kaarsholm, N. C.; Lee, R. W.-K.; Dunn, M. F. *Biochemistry* **1991**, *30*, 6636–6645.
(27) We note that simulations of observed ESR signals provide a useful means of estimating the spectral parameters but do not necessarily produce unique fits.
(28) Nilges, M. J. Ph.D. Thesis, University of Illinois, Urbana, Illinois, 1979.

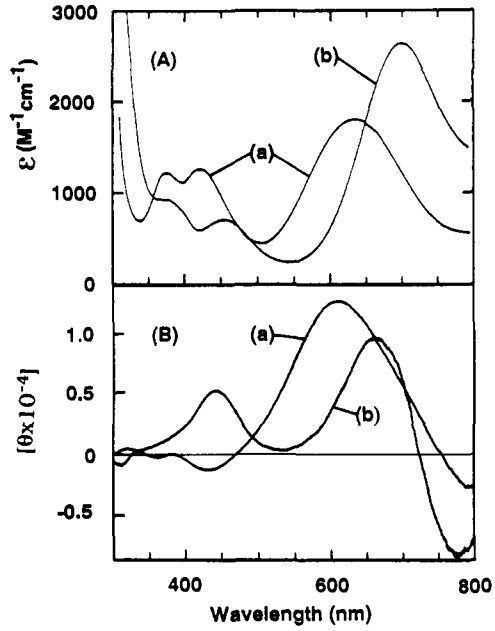

Figure 2. UV-visible electronic absorption spectra (A) and circular dichroism spectra (B) of the Cu(II)-R_6-thiolate complexes formed with tetrafluorobenzenethiolate (a) and benzenethiolate (b). Spectra were recorded on solutions of hexamer complexes prepared in 50 mM Tris-ClO_4 buffer, pH 7.5, incorporating a 0.2×10^{-3} M concentration of copper sites.

Raman spectrometer equipped with Ar and Kr ion lasers and a 1024 channel intensified diode array. Spectra were recorded immediately following the preparation of the Cu(II)-R_6-PFBT complex in the presence of 100 mM phenol at pH 8. The M/thiolate ratio was 1:1.

Results

Cu(II)-R_6-Thiolate Electronic and CD Spectra. UV-visible electronic absorption spectral data for a series of Cu(II)-R_6-thiolate complexes are presented in Table I. The spectra of the TFBT and BT complexes are presented in Figure 2A. The data of Table I show that the Cu(II)-R_6-thiolate complexes all give electronic absorption spectra which display a single intense charge-transfer (CT) band in the region 600–700 nm. This band is flanked by bands in the 300–450 nm region and an additional band at approximately 900 nm. The data (Table I) establish that the energy of the prominent visible CT band is strongly influenced by the nature of the thiolate ligand. This band is analogous to the intense absorption that occurs in the 600–630 nm region of blue copper protein spectra and is assigned as an S(thiolate)–Cu(II) ligand-to-metal CT (LMCT) transition. The low energy of the band at ~900 nm supports its assignment as a ligand field (d–d) transition attributable to a near tetrahedrally coordinated Cu(II) ion. The bands in the 300–450 nm region probably arise from π(ImH)–Cu(II) LMCT transitions. Comparable transitions have been identified in the spectra of blue copper proteins and in the spectra of various small molecule Cu(II)–imidazole chromophores.[10]

The CD spectra of Cu(II)-R_6-TFBT and Cu(II)-R_6-BT are shown in Figure 2B. The 696-nm CT band in the optical spectrum of Cu(II)-R_6-BT is resolved into positive (664 nm) and negative (780 nm) CD bands. These CD bands are attributable to π-(S)–Cu(II) and σ(S)–Cu(II) LMCT transitions. This interpretation is in accordance with theory, which predicts[29] that the CD bands associated with the π and σ CT transitions will have opposite signs. The 630-nm optical CT band in Cu(II)-R_6-TFBT appears as a large positive CD band at 611 nm and an incompletely distinguished minor negative band at >750 nm. A comparison of the Cu(II)-R_6-TFBT and Cu(II)-R_6-BT CD spectra indicates that the π and σ components of the S(thiolate)–Cu(II) LMCT envelope are quite different in each complex, reflecting the different character of the respective Cu(II)–S(thiolate) bonds. The CD spectral data for the Cu(II)-R_6-thiolate complexes formed with PFBT, TFBT, BT, and 4-MeBT are summarized in Table II.

(29) Ibarra, C.; Soto, R.; Adan, L.; Decinti, A.; Bunei, S. *Inorg. Chim. Acta* **1972**, *6*, 601–606.

Table II. Circular Dichroism Spectral Data[a] for the Cu(II)-R_6-Thiolate Complexes

thiolate[b]	
PFBT	322 (+0.092), 364 (–0.040), 428 (–0.165), 607 (+1.19)
TFBT	320 (+0.034), 362 (–0.026), 433 (–0.127), 611 (+1.25)
BT	312 (–0.085), 375[c] (+0.116), 442 (+0.522), 664 (+0.937), 780 (–0.810)
4-MeBT[d]	320 (+), 380[c] (+), 446 (+), 673 (+), 780 (–)

[a] λ_{max}, nm ($[\theta] \times 10^{-4}$). [b] BT = benzenethiolate, PFBT = pentafluorobenzenethiolate, TFBT = tetrafluorobenzenethiolate, 4-MeBT = 4-methylbenzenethiolate. [c] Broad, unresolved shoulder. [d] Rapid reduction of this complex precluded measurement of $[\theta]$ values.

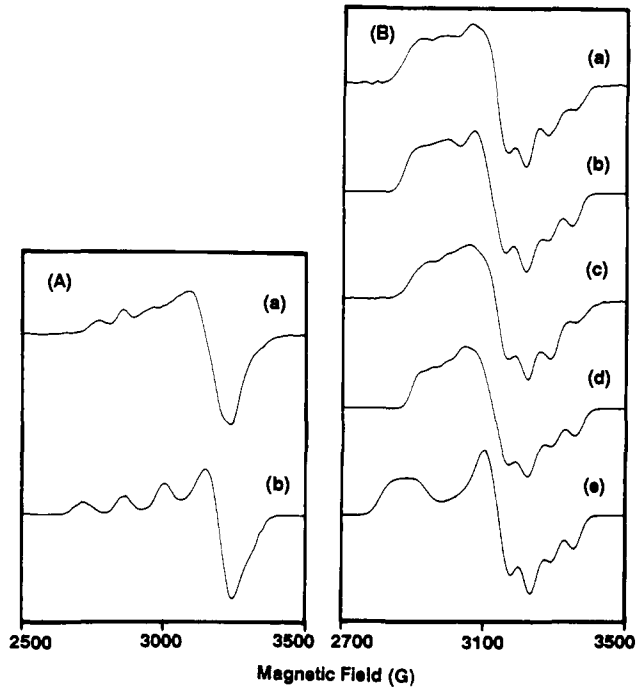

Figure 3. X-band ESR spectra (110 K) (A) of the Cu(II)-R_6-thiolate complexes formed with pentafluorobenzenethiolate (PFBT) (a) and 2-pyridinethiolate (2-PT) (b). The spectra were recorded on a solution of hexamer complex prepared in 50 mM Tris-ClO_4 buffer, pH 7.5, incorporating a 0.4×10^{-3} M concentration of copper sites. X-band ESR spectra (110 K) (B) of the Cu(II)-R_6-thiolate complexes formed with benzenethiolate (BT) (a) and 4-methylbenzenethiolate (4-MeBT) (c). Spectra were recorded on solutions of hexamer complexes prepared in 50 mM Tris-ClO_4 buffer, pH 7.5, incorporating a 0.4×10^{-3} M concentration of copper sites. Simulations of spectra a and c are shown in b and d, respectively. The spectrum of stellacyanin, simulated using the parameters of Gewirth et al. (ref 30), is shown in e for comparison.

ESR Spectra. The ESR spectra of the Cu(II)-R_6-thiolate complexes are presented in Figure 3. The spectrum of the PFBT complex (Figure 3A, spectrum a) is virtually identical to that of the TFBT complex (not shown). The spectra of the complexes formed with BT and 4-MeBT are shown in Figure 3B (spectra a and c, respectively). Spectra b and d of Figure 3B are the respective simulations of spectra a and c that are obtained using the parameters shown in Table III. The spectrum of the complex formed with 2-pyridinethiolate (2-PT) is shown in Figure 3A (spectrum b). The ESR spectral parameters are summarized in Table III along with literature values for azurin, plastocyanin, stellacyanin, cucumber basic protein (CBP), and Cu(II)-substituted liver alcohol dehydrogenase (Cu(II)-LADH).

The Cu(II) ESR signal is affected dramatically by the nature of the thiolate group ligated to the Cu(II) ion (Figure 3). No ligand hyperfine couplings are observed. The spectrum of Cu(II)-R_6-PFBT (Figure 3A, a) exhibits a resolved copper hyperfine

Table III. ESR Parameters

species[a]	g_x	$(A_x)^b$	g_y	$(A_y)^b$	g_z	$(A^z)^b$
Cu(II)-R_6-PFBT	2.065	(27)	2.065	(27)	2.264	(87)
Cu(II)-R_6-TFBT	2.065	(27)	2.065	(27)	2.264	(87)
Cu(II)-R_6-BT[c]	2.025	(60)	2.090	(33)	2.230	(38)
Cu(II)-R_6-4-MeBT[c]	2.020	(60)	2.090	(32)	2.210	(42)
Cu(II)-R_6-2-PT	2.060		2.060		2.240	(152)
stellacyanin[c,d]	2.018	(57)	2.077	(29)	2.287	(35)
azurin[e]	2.059		2.059		2.255	(60)
plastocyanin[f]	2.042		2.059		2.226	(63)
CBP[g]	2.02	(60)	2.08	(10)	2.207	(55)
Cu(II)-LADH[h]	2.030	(76)	2.060	(30)	2.210	(50)

[a] BT = benzenethiolate, PFBT = pentafluorobenzenethiolate, TFBT = tetrafluorobenzenethiolate, 4-MeBT = 4-methylbenzenethiolate, 2-PT = 2-pyridinethiolate, Cu(II)-CBP = cucumber basic protein, LADH = the copper-substituted derivative of liver alcohol dehydrogenase. [b] In $cm^{-1} \times 10^4$. [c] Values employed in ESR simulations, Figure 4. [d] From ref 30. [e] From ref 9. [f] From ref 5. [g] From ref 2h. [h] From ref 45b,d.

Table IV. Circular Dichroism Spectral Data[a] for the Co(II)-R_6-Thiolate Complexes

thiolate[b]	
PFBT	302 (+1.12), 330 (+0.940), 386 (+0.283), 566 (+0.031), 605 (−0.152)
TFBT	301 (+1.68), 329 (+1.17), 383 (+0.355), 396[c] (+0.323), 561 (+0.031), 599 (−0.139)
BT	309 (+1.78), 344[c] (+0.570), 397 (+0.598), 453 (−0.025), 517 (+0.067), 598 (−0.151), 637 (+0.036)
4-MeBT	306 (+1.76), 355 (+0.586), 397 (+0.794), 450 (−0.083), 517 (+0.116), 590 (−0.400), 634 (+0.130)

[a] λ_{max}, nm ($[\theta] \times 10^{-4}$). [b] PFBT = pentafluorobenzenethiolate, TFBT = tetrafluorobenzenethiolate, BT = benzenethiolate, 4-MeBT = 4-methylbenzenethiolate. [c] Shoulder.

splitting in the $g_\parallel$ region, giving $A_\parallel = 87 \times 10^{-4}$ cm^{-1}, and corresponds to a Cu(II) ion possessing a $d_{x^2-y^2}$ ground state ($g_\parallel > g_\perp > 2$). This spectrum also appears to be approximately axial; however, we note that small rhombic deviations ($g_x \neq g_y$, $A_x \neq A_y$) in the ESR spectra of copper proteins are not resolved efficiently by the X-band experiment. The ESR spectra of Cu(II)-R_6-BT (Figure 3B, a) and Cu(II)-R_6-4-MeBT (Figure 3B, c) appear very different from that of Cu(II)-R_6-PFBT. In each case, the copper hyperfine coupling is only partially resolved. Our simulations indicate that it is necessary to invoke rhombic g tensors to obtain reasonable agreement with the experimental data. Several features of these spectra are noteworthy. The largest hyperfine coupling does not occur along the same magnetic axis as the largest g value, and the A_z values are very small, viz., $<50 \times 10^{-4}$ cm^{-1}. In these respects, the spectra of Cu(II)-R_6-BT and Cu(II)-R_6-4-MeBT show an intriguing parallel to the ESR spectrum[11,12,14,30] of stellacyanin. A simulation of this latter spectrum[30] is presented in Figure 3B (spectrum e) for comparison. The g_x and g_y regions of the Cu(II)-R_6-BT and Cu(II)-R_6-4-MeBT spectra are strikingly similar to that of the stellacyanin spectrum; the major difference is the larger value of g_z for the latter spectrum.

Cobalt(II)-R_6-Thiolate CD Spectra. The UV-visible absorption spectra of the Co(II)-R_6-thiolate complexes[16,26] are very similar to those of the Co(II)-substituted derivatives[31] of azurin, plastocyanin, and stellacyanin. In the 500–650 nm region, the Co(II)-R_6-thiolate spectra display intense d–d bands ($\epsilon > 500$ M^{-1} cm^{-1}) attributable to low symmetry-split components of the $^4A_2$–$^4T_1$(P) transition. This splitting is characteristic of the high-spin Co(II) ion in a distorted tetrahedral ligand field.[32,33] Additional bands arising from S(thiolate)–Cu LMCT transitions

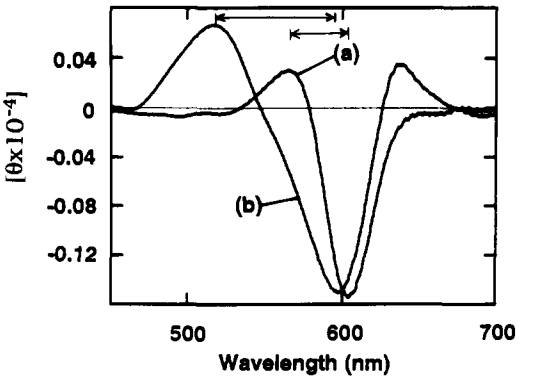

Figure 4. Circular dichroism spectra of the Co(II)-R_6-thiolate complexes formed with pentafluorobenzenethiolate (PFBT) (a) and benzenethiolate (BT) (b). Spectra were recorded on solutions of hexamer complexes prepared in 50 mM Tris–ClO_4 buffer, pH 8.0, incorporating a 0.9×10^{-3} M concentration of copper sites. The arrows indicate the splittings between the visible CD bands.

are observed at higher energy. Table IV summarizes the UV-visible CD spectra of several Co(II)-R_6-thiolate complexes. The CD associated with the d–d envelope reflects the inherent molecular asymmetry of the metal environment. Our CD results show that considerably different splittings of the d–d bands occur for the Co(II)-R_6-thiolate complexes studied. This is illustrated by the CD spectra of Co(II)-R_6-BT and Co(II)-R_6-PFBT, which are presented in Figure 4. The energy separations between the largest positive and negative bands of the d–d envelope are 2600 cm^{-1} for Co(II)-R_6-BT and 1100 cm^{-1} for Co(II)-R_6-PFBT. For Co(II)-R_6-4-MeBT and Co(II)-R_6-TFBT, the corresponding values are 2400 and 1100 cm^{-1}, respectively. These results indicate that the Co(II) geometries in Co(II)-R_6-BT and Co(II)-R_6-4-MeBT differ significantly from those in Co(II)-R_6-PFBT and Co(II)-R_6-TFBT.

Pentacoordinate Cu(II). To investigate the effects of pentacoordination at the Cu(II) site, we have studied the Cu(II)-R_6 complexes formed with the ambidentate ligands 2-PT and 4-PT. The electronic absorption spectra of these two complexes appear very different (Table I). The intense low-energy S–Cu(II) LMCT band (λ_{max} = 646 nm, ϵ = 1250 M^{-1} cm^{-1}) that dominates the optical spectrum of Cu(II)-R_6-4-PT is analogous to those of the monodentate thiolate complexes. Notably, this feature is absent in the spectrum of Cu(II)-R_6-2-PT. Furthermore, the ESR spectrum of Cu(II)-R_6-2-PT (Figure 3A, b) is characterized by a large $A_\parallel$ value of 152×10^{-4} cm^{-1}, which is representative of a normal tetragonal or five-coordinate Cu(II) site. The absence of a prominent S(thiolate)–Cu(II) LMCT absorption indicates that this complex does not possess an S(thiolate)–Cu(II) bond or, at most, that the S(thiolate)–Cu(II) interaction is very weak. Due to sample instability we were unable to record the ESR spectrum of the Cu(II)-R_6-4-PT complex. Our studies[26] of the Co(II)-R_6 complexes of these two isomers indicate that 2-PT acts as an N,S bidentate chelator[34,35] that forms a pentacoordinate $Co^{II}N_4S$ arrangement. In contrast, 4-PT behaves much like BT and coordinates via the thiolate sulfur, forming a pseudotetrahedral $Co^{II}N_3S$ geometry. The present results indicate that analogous Cu(II) complexes are formed with 2-PT and 4-PT (Table I). The band at 720 nm in the spectrum of Cu(II)-R_6-2-PT is assigned to a Cu(II) d–d transition. This band occurs at much higher energy than the d–d band of Cu(II)-R_6-4-PT, which occurs at ~900 nm. Similar d–d bands are obtained for the Cu(II)-R_6 complexes containing monodentate thiolate ligands, whereas the higher energy of the 720-nm band reflects the stronger ligand field associated with a more flattened geometry. We propose that the Cu(II) site in Cu(II)-R_6-2-PT comprises a pentacoordinate $Cu^{II}N_4S$ arrangement in which the Cu(II)–S interaction is weak

(30) Gewirth, A. A.; Cohen, S. L.; Schugar, H. J.; Solomon, E. I. *Inorg. Chem.* **1987**, *26*, 1133–1146.
(31) Solomon, E. I.; Rawlings, J.; McMillin, D. R.; Stephens, P. J.; Gray, H. B. *J. Am. Chem. Soc.* **1976**, *98*, 8046–8048.
(32) Coleman, J. E.; Coleman, R. V. *J. Biol. Chem.* **1972**, *247*, 4718–4728.
(33) Flamini, A.; Sestili, L.; Furlani, C. *Inorg. Chim. Acta* **1971**, *5*, 241–246.
(34) Mura, P.; Olby, B. G.; Robinson, S. D. *J. Chem. Soc., Dalton Trans.* **1985**, 2101–2112.
(35) Kitagawa, S.; Munakata, M.; Shimono, H.; Matsuyama, S.; Masuda, H. *J. Chem. Soc., Dalton Trans.* **1990**, 2105–2109.

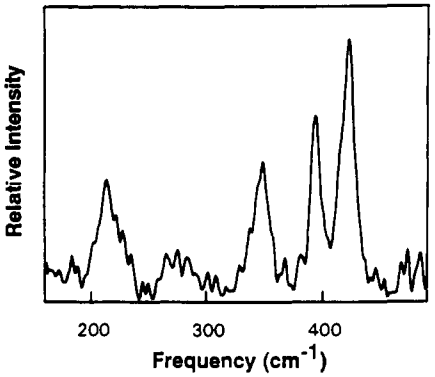

Figure 5. Resonance Raman spectrum of the Cu(II)-R_6-thiolate complex formed with pentafluorobenzenethiolate using a laser excitation wavelength of 647.1 nm. The spectrum was recorded on a solution of hexamer complex prepared in 50 mM Tris-ClO_4 buffer, pH 8.0, incorporating a 0.7×10^{-3} M concentration of copper sites. Other parameters are as follows: 50 mW laser power incident on the sample; 2.2 cm^{-1} bandwidth; sum of 256 scans; a 9-point binomial smoothing function was applied.

and, therefore, does not give rise to an intense S-Cu(II) LMCT in the visible region.

Resonance Raman Spectroscopy. The resonance Raman spectrum of the Cu(II)-R_6-PFBT complex is presented in Figure 5. The spectrum possesses dominant features at 422, 393, 348, and 213 cm^{-1}. Control experiments performed in the absence of copper determined that bands other than those from the Cu(II)-R_6-PFBT complex did not occur in this region. When the solution of Cu(II)-R_6-PFBT was irradiated with a laser excitation wavelength of 514 nm (noncoincident with the 626-nm LMCT band), these features were not observed. Therefore, we conclude that these vibrations show strong intensity enhancement via resonance with the 626-nm S-Cu(II) LMCT band. We note that there is an impressive similarity between this spectrum and that of azurin[36] (from *Pseudomonas aeruginosa*), which possesses intense bands at 424, 404, and 369 cm^{-1} and a less intense band at 261 cm^{-1}.

Discussion

Metal Environment. The crystal structures[21,22] of two Zn(II)-R_6 hexamer complexes show that the metal chelate site is formed by three symmetry-related HisB10 imidazolyl groups. Distorted tetrahedral (C_{3v}) Zn(II) coordination geometries are completed by either a chloride ion[21] or a phenolate anion[22] from solution which resides on the 3-fold symmetry axis of the hexamer. The extent of similarity between the coordination properties of the Zn(II) center in the Zn(II)-R_6 hexamer and the Cu(II) ions of the Cu(II)-R_6 hexamer is unclear. Our studies[16,26,37,38] of Co(II)-R_6 adducts formed with a wide variety of ligands show that the Co(II)-R_6 hexamer possesses a distinct preference for the formation of pseudotetrahedral $Co^{II}N_3L$ geometries.[26] This preference probably arises from the combination of a relatively constrained protein chelate site and the narrow channel from the metal ion to the exterior solution, which limits possible orientations of the fourth exogenous ligand and sterically averts the coordination of a fifth ligand. These structural characteristics account for the observation that the insulin hexamer can overcome the ligand-field-driven distortion of the Cu(II) ion to the familiar square planar geometry and concomitantly stabilize the Cu(II)-thiolate interaction in the Cu(II)-R_6-thiolate complexes. Therefore, the type 1 Cu(II) centers of these complexes likely consist of distorted tetrahedral $Cu^{II}N_3(RS^-)$ arrangements (Figure 1).

Electronic Spectra. The optical and ESR parameters of the Cu(II)-R_6-thiolate complexes exhibit characteristics that are quite different from those observed for normal tetragonal Cu(II) complexes. These latter Cu(II) sites give rise to weakly intense visible absorption spectra ($\epsilon < 100$ M^{-1} cm^{-1}) and large ESR hyperfine coupling constants[1c] ($A_\parallel = (130\text{–}220) \times 10^{-4}$ cm^{-1}). The intense visible CT bands and small ESR hyperfine values of the Cu(II)-R_6-thiolate complexes fall within the domain of type 1 spectral features.

The energy of the prominent CT band clearly is very sensitive to the electron-withdrawing nature of the substituent in the benzenethiolate group. Ring substitution is expected to shift the energies of the sulfur lone pair p orbitals relative to that of the Cu(II) $d_{x^2-y^2}$ orbital. The thiolate sulfur lone pairs may overlap with the Cu(II) $d_{x^2-y^2}$ orbital to produce π(S)-Cu(II) and σ(S)-Cu(II) LMCT transitions. The intensities of these transitions will be related to the degree of overlap between the sulfur and copper orbitals. A determination of the relative contributions made by the π(S)-Cu and σ(S)-Cu LMCT transitions to the CT envelope in type 1 copper chromophores is difficult, but it remains a topic of considerable current interest. More detailed studies of the Cu(II)-R_6-thiolate complexes will be necessary to achieve an unambiguous assignment of the CT spectra.

The ESR data show that the ESR signal is extremely sensitive to the nature of the substituent on the aromatic ring of the benzenethiolate group. The qualitative appearances of the spectra of Cu(II)-R_6-BT (Figure 3B, a) and Cu(II)-R_6-4-MeBT (Figure 3B, c) are very similar. The rhombic nature of these spectra indicates that the protein imposes very distorted geometries upon the Cu(II) ions. In each case, abnormally large hyperfine couplings occur along g_x and g_y, and the largest coupling does not occur along g_z. The ESR spectrum of stellacyanin is similar, viz., Figure 3B, e. The axial ESR spectra obtained for the PFBT and TFTP Cu(II)-R_6 complexes versus the rhombic spectra obtained for BT and 4-MeBT are intriguing. The dissimilarity of the respective g and A tensors for the axial and rhombic spectra indicates that the ESR signals of Cu(II)-R_6-PFBT and Cu(II)-R_6-TFBT arise from Cu(II) geometries which are different from those of Cu(II)-R_6-BT and Cu(II)-R_6-4-MeBT. Although similar in steric bulk, the donor properties of the four thiolates are expected to be quite different. The more polarizable BT sulfur atom is expected to form a more covalent bond with Cu(II) than is the PFBT sulfur and hence should generate a stronger ligand field. This increased ligand field strength at the fourth coordination position is the probable origin of the alteration in site symmetry that is evidenced by the change from near-axial ESR spectra for Cu(II)-R_6-PFBT and Cu(II)-R_6-TFBT to rhombic spectra for Cu(II)-R_6-BT and Cu(II)-R_6-4-MeBT. These results are in agreement with predictions[30] that the introduction of a ligand producing an increased ligand field strength at the methionine position in the Cu(II) coordination sphere of plastocyanin could cause a change from an effective C_{3v} site symmetry to an effective C_{2v} site symmetry and thus would account for the different ESR characteristics of plastocyanin versus stellacyanin.

Coordination of the bidentate ligand, 2-pyridinethiolate, abolishes the type 1 copper spectral features, reaffirming that both strong Cu(II)-thiolate ligation and an appropriate Cu(II) coordination geometry are prerequisites for the type 1 characteristics. We note that the ESR spectrum of Cu(II)-R_6-2-PT (Figure 3A, b; Table III) is similar to that of Cu-Zn bovine superoxide dismutase[39] (SOD) (for ^{63}Cu: $g_x = 2.03$, $g_y = 2.09$, $g_z = 2.26$, $A_x = 52 \times 10^{-4}$ cm^{-1}, $A_y = 35 \times 10^{-4}$ cm^{-1}, $A_z = 142 \times 10^{-4}$ cm^{-1}). The SOD crystal structure[40] shows that each Cu(II) ion is coordinated by the imino nitrogens of four histidines in an approximately square plane possessing a limited tetrahedral distortion. An axially coordinated water molecule completes a pentacoordinate arrangement. The optical absorption spectrum of Cu(II)-R_6-2-PT (Table I) is also comparable to that of SOD.

(36) Thamann, T. J.; Frank, P.; Willis, L. J.; Loehr, T. M. *Proc. Natl. Acad. Sci. U.S.A.* **1982**, *79*, 6396–6400.
(37) Roy, M.; Brader, M. L.; Lee, R. W.-K.; Kaarsholm, N. C.; Hansen, J. F.; Dunn, M. F. *J. Biol. Chem.* **1989**, *264*, 19081–19085.
(38) Brader, M. L.; Kaarsholm, N. C.; Dunn, M. F. *J. Biol. Chem.* **1990**, *265*, 15666–15670.
(39) Lieberman, R. A.; Sands, R. H.; Fee, J. A. *J. Biol. Chem.* **1982**, *257*, 336–344.
(40) Tainer, J. A.; Getzoff, E. D.; Richardson, D. C. In *2SOD: Cu, Zn-Superoxide Dismutase Complete Atomic Coordinates*; Richardson, D. C., Richardson, J. S., Eds.; Brookhaven Protein Structure Data Bank: Brookhaven, NY, 1980.

The SOD spectrum[41] is characterized by a d–d band at 680 nm and a poorly resolved shoulder at 430 nm.

Comparisons with Blue Copper Proteins. The crystal structures of azurin[2c] and plastocyanin[2f] define closely analogous copper chelate sites in which two His nitrogens, a Cys sulfur, and the copper form an approximately trigonal plane with a long axial bond to the Met sulfur. The ESR and optical parameters of azurin and plastocyanin are very similar. The ESR spectrum of azurin[9] is axial ($A_\parallel = 60 \times 10^{-4}$ cm^{-1}), whereas that of plastocyanin[5] exhibits a very slight rhombic distortion ($g_x - g_y = 0.017$ and $A_\parallel = 63 \times 10^{-4}$ cm^{-1}). The ESR spectrum of Cu(II)-R_6–PFBT (Figure 3A, a) is close to axial and appears qualitatively similar to those of azurin and plastocyanin. The value of $A_\parallel$, 87×10^{-4} cm^{-1}, is slightly larger than those of most blue copper proteins, but it is significantly smaller than the values observed for tetragonal Cu(II) sites[1c] ($A_\parallel > 130 \times 10^{-4}$ cm^{-1}). Single-crystal spectral studies in conjunction with ligand field calculations indicate that an approximately elongated C_{3v} geometry with slight rhombic distortion is appropriate for the Cu(II) site of plastocyanin.[4] The zinc sites defined by the Zn(II)-R_6 hexamer crystal structures[21,22] possess C_{3v} symmetry, and thus the Cu(II) site symmetry in Cu(II)-R_6–PFBT likely is similar to those of plastocyanin and azurin.

The stellacyanin ESR spectrum is unusual and quite different from those of azurin and plastocyanin (Table III); g_z is very small (35×10^{-4} cm^{-1}) and there is substantial rhombic splitting ($g_x = 2.018$, $g_y = 2.077$).[14] Furthermore, the largest hyperfine coupling is associated with the smallest g value, whereas this feature is usually associated with the largest g value. Collectively, the stellacyanin spectroscopic and theoretical studies show that this unusual hyperfine tensor is related more intimately to the symmetry of the Cu(II) ion than to the actual nature of the donor atoms.[14,30] The Cu(II) site of stellacyanin is predicted[14,30] to possess a C_{2v} effective symmetry (flattened tetrahedral), whereas plastocyanin and azurin exhibit approximate C_{3v} effective symmetry. The primary structure and spectroscopic properties of the cucumber basic blue protein (CBP) are closely comparable to those of stellacyanin. A low-resolution structure[2h] of CBP has shown that the Cu(II) site of CBP incorporates the prototypical blue copper ligands, [(His)$_2$(Met)(Cys)], attesting to the capability of this ligand set to generate the stellacyanin-like ESR and CT characteristics. Although the bonding parameters of the CBP Cu(II) site were not available in this study,[2h] this result was consistent with deductions that the unusual ESR spectrum of stellacyanin was intrinsically related to specific geometrical characteristics of the copper site.[14,30] The qualitative commonality of the rhombic ESR signals for Cu(II)-R_6–BT, Cu(II)-R_6–4-MeBT, CBP, and stellacyanin suggests that the Cu(II) geometries in these systems are related. A relatively intense optical absorption feature at ~450 nm[2h,3] also distinguishes stellacyanin and CBP from plastocyanin and azurin. The CD spectrum of Cu(II)-R_6–BT (Figure 2B) also shows a relatively intense band in this region (442 nm), a feature not present in the CD spectra of Cu(II)-R_6–PFBT or Cu(II)-R_6–TFBT.

The diversity of the electronic spectral characteristics exhibited by the Cu(II)-R_6–thiolate complexes studied herein indicates that the Cu(II)–S(thiolate) linkage plays a major role in defining the electronic structure of the Cu(II) ion in a pseudotetrahedral ligand field. Our results suggest that the manifestation of stellacyanin-like rhombic ESR characteristics in these Cu^{II}N$_2$S(thiolate) chromophores is mediated by an enhancement of the covalency of the Cu(II)–S(thiolate) interaction.

Cobalt(II) Substitution. Studies of the cobalt(II)-substituted derivatives of blue copper proteins have provided valuable insight into the nature of the metal sites.[31,42,43] Studies of the d–d bands in high-spin Co(II) complexes show that the splitting of the $^4A_2$–$^4T_1$(P) transition provides a qualitative indication of the degree of distortion from tetrahedral symmetry.[32,33] The splitting between the d–d components is much greater for the Co(II)-R_6–BT and Co(II)-R_6–4-MeBT spectra than for the Co(II)-R_6–PFBT and Co(II)-R_6–TFBT spectra. These results suggest that greater distortions from tetrahedral symmetry occur in the Co(II)-R_6–BT and Co(II)-R_6–4-MeBT complexes than in the Co(II)-R_6–PFBT and Co(II)-R_6–TFBT complexes. These observations are paralleled by the finding that the Cu(II)-R_6 BT and 4-MeBT complexes give rhombic ESR spectra, whereas those with PFBT and TFBT give axial spectra. It is unlikely that a direct correspondence exists between the Co(II) and Cu(II) geometries in the respective M(II)-R_6–thiolate complexes.[44] Nevertheless, the Co(II) CD data are in agreement with the observation that the fluorinated and nonfluorinated thiolate ligands give Cu(II)-R_6 complexes with different geometries.

Resonance Raman Spectroscopy. The resonance Raman experiment represents a sensitive method for probing the Cu(II) environment in the type 1 chromophore. Blue copper proteins show several intense bands in the region 350–450 cm^{-1} with which intensity enhancement occurs via resonance with the ~600-nm LMCT band.[8,9,36] These bands have been attributed to highly coupled Cu(II)–S(Cys) and Cu(II)–N(Im) stretching modes.[36] The resonance Raman spectrum presented in Figure 5 provides further vindication that the Cu(II) site of Cu(II)-R_6–PFBT embodies bonding characteristics that are fundamentally similar to those of the blue copper proteins. We infer that the Cu(II)–S interaction in Cu(II)-R_6–PFBT is probably closely comparable to the 2.1-Å Cu(II)–S(cysteine) bonds identified in azurin[2c] and plastocyanin.[2f]

Other Type 1 Cu(II) Model Systems. The Cu(II)-substituted derivative of the zinc enzyme, liver alcohol dehydrogenase (LADH), exhibits all the spectral features of a type 1 Cu(II) site.[45] The Cu(II) ion of Cu(II)-LADH is presumed to coordinate two Cys thiolates, a His imidazole, and a water or hydroxyl oxygen. The ESR spectrum of Cu(II)-LADH possesses rhombic character and unusual hyperfine splittings (Table III) similar to the Cu(II)-R_6–BT and Cu(II)-R_6–4-MeBT complexes. The more complex resonance Raman spectrum[45e,f] of Cu(II)-LADH is probably a consequence of the two Cu(II)–cysteine linkages per site.

The only example of a small molecule complex that gives the type 1 CT and ESR spectral features is a complex in which a Cu(II)–S(thiolate) interaction with 2-methyl-2-propanethiolate is stabilized at 77 K with the hindered N_3 tridentate pyrazolylborate ligand, hydrotris(3,5-diisopropyl-1-pyrazolyl)borate.[46] This complex is suggested[46] to possess a tetrahedral Cu^{II}N$_3$S geometry. The ESR ($A_\parallel = 72 \times 10^{-4}$ cm^{-1}) and optical properties ($\lambda_{max} = 608$ nm, $\epsilon > 3500$ M^{-1} cm^{-1}) are similar to those of the Cu(II)-R_6–PFBT complex. The 3-fold symmetry of the tris(pyrazolyl)borate ligand makes it somewhat analogous to the HisB10 chelate site of the R_6 insulin hexamer. In view of the structural and spectral parallels, it is possible that the Cu(II) sites of the Cu(II)-R_6–PFBT complex and the tris(pyrazolyl)borate–Cu(II)–2-methyl-2-propanethiolate complex are geometrically quite similar.

Conclusions

Our results show that Cu(II)-R_6–thiolate complexes successfully model the prominent optical, ESR, and resonance Raman features

(41) Weser, U. *Struct. Bonding (Berlin)* **1973**, *17*, 1–65.
(42) McMillin, D. R; Holwerda, R. A.; Gray, H. B. *Proc. Natl. Acad. Sci. U.S.A.* **1974**, *71*, 1339–1341.
(43) McMillin, D. R.; Rosenberg, R. C.; Gray, H. B. *Proc. Natl. Acad. Sci. U.S.A.* **1974**, *71*, 4760–4762.
(44) (a) *Zinc Enzymes, Progress in Inorganic Biochemistry and Biophysics*; Bertini, I., Luchinat, C., Maret, W., Zeppezauer, M., Eds.; Birkhauser: Basel, 1986; Vol. 1, pp 1–640. (b) Bertini, I.; Luchinat, C.; Viezzoli, M. S. In *Zinc Enzymes*; Bertini, I., Luchinat, C., Maret, C., Zeppezauer, M., Eds.; Birkhauser: Stuttgart, 1986; pp 27–47.
(45) (a) Maret, W.; Dietrich, H.; Ruf, H.; Zeppezauer, M. *J. Inorg. Biochem.* **1980**, *12*, 241–252. (b) Maret, W.; Zeppezauer, M.; Desideri, A.; Morpurgo, L.; Rotilio, G. *Biochim. Biophys. Acta* **1983**, *743*, 200–206. (c) Dietrich, H.; Maret, W.; Kozlowski, H.; Zeppezauer, M. *J. Inorg. Biochem.* **1981**, *14*, 297–311. (d) Maret, W.; Kozlowski, H. *Biochim. Biophys. Acta* **1987**, *912*, 329–337. (e) Maret, W.; Shiemke, A. K.; Wheeler, W. D.; Loehr, T. M.; Sanders-Loehr, J. *J. Am. Chem. Soc.* **1986**, *108*, 6351–6359. (f) Maret, W.; Zeppezauer, M.; Sanders-Loehr, J.; Loehr, T. M. *Biochemistry* **1983**, *22*, 3202–3206.
(46) Kitajima, N.; Fujisawa, K.; Moro-oka, Y. *J. Am. Chem. Soc.* **1990**, *112*, 3210–3212.

of blue copper proteins that are considered fundamental signatures of biological structure and function. The spectral properties of these complexes are influenced strongly by the nature of the thiolate ligand. Substitution in the aromatic ring of benzenethiolate affects the donor properties of the sulfur atom, thereby altering the covalency of the Cu(II)-S interaction. This change in character of the Cu(II)-S(thiolate) bond appears to be the principal cause of perturbations of the Cu(II) site symmetry. These model studies demonstrate that an increase in the covalency of the Cu(II)-S(thiolate) linkage in a pseudotetrahedral $Cu^{II}N_3S$(thiolate) environment can cause the ESR signal to change from one that is qualitatively similar to those of plastocyanin and azurin to one that is qualitatively similar to that of stellacyanin.

The C_{3v} symmetry of the Zn(II) sites in the Zn(II)-R_6 crystal structures[21,22] renders plausible the possibility that a similar geometry may be obtained for some of the Cu(II)-R_6-thiolate derivatives. In view of the spectral similarities that exist between Cu(II)-R_6-PFBT, Cu(II)-R_6-TFBT, azurin, plastocyanin, and the complex tris(pyrazolyl)borate-Cu(II)-2-methyl-2-propanethiolate, we suggest that an approximate C_{3v} geometry is probable for the Cu(II) ion in the Cu(II)-R_6-PFBT and Cu(II)-R_6-TFBT complexes. In contrast, the Cu(II) sites in the Cu(II)-R_6-BT and Cu(II)-R_6-4-MeBT complexes, which give rise to rhombic ESR spectra, appear to be more closely related to the Cu(II) site in stellacyanin, which is predicted[14,30] to possess an effective C_{2v} geometry.

Acknowledgment. We are grateful to the Novo Research Institute (Denmark) for the provision of insulin. We thank Dr. Ole Hvilsted Olsen for providing the computer graphics image of insulin and Professor Guy Dodson for permission to reproduce it. This work was supported by NIH Grant 5-R01-DK 42124-02. The laser Raman instrumentation was purchased with funds from NSF Grant CHE 8805482. ESR analysis software was furnished by the Illinois ESR Research Center, NIH Division of Research Resources, Grant No. RR01811.

Endoperoxide Formation of Helianthrene with Triplet Molecular Oxygen. A Spin-Forbidden Reaction

M. Seip and H.-D. Brauer*

Contribution from the Institut für Physikalische und Theoretische Chemie, Universität Frankfurt, Niederurseler Hang, D 6000 Frankfurt/Main, FRG. *Received October 28, 1991*

Abstract: Dibenzo[*a*,*o*]perylene (helianthrene = HEL), known to be a very reactive singlet molecular oxygen ($^1O_2$, $^1\Delta_g$) acceptor, also reacts with molecular oxygen in its triplet ground state ($^3O_2$, $^3\Sigma_g^-$) to form helianthrene endoperoxide (HELPO). The thermal endoperoxide formation was studied in several solvents at room temperature. In nonpolar solvents such as toluene and carbon disulfide the temperature-dependent equilibrium, HEL + $^3O_2$ ⇄ HELPO, is established by the thermolysis of HELPO even at low temperatures. Kinetic parameters for the HELPO formation in toluene are $\Delta H^{\ddagger} = 10.2 \pm 1.0$ kcal mol^{-1} and $\Delta S^{\ddagger} = -39 \pm 5$ eu, indicating that $^1O_2$ is not involved in the reaction pathway. This is the first example of aromatic endoperoxide formation by reaction with molecular oxygen in its ground state.

Introduction

Helianthrene (HEL) is one of the most reactive $^1O_2$ acceptors known. Measurements of the self-sensitized or methylene blue sensitized photooxygenation have shown that HEL reacts with $^1O_2$ near the diffusion-controlled limit to form the endoperoxide HELPO[1,2] (see Figure 1).

During the investigation of its photooxygenation, it was observed that HEL also reacted with molecular oxygen in the dark. Preliminary tests surprisingly indicated that this dark reaction also led to the formation of HELPO. Such a spin-forbidden reaction between an aromatic compound with a singlet ground state and molecular oxygen in its ground state ($^3O_2$) leading to the endoperoxide with a singlet ground state has—to our knowledge—not previously been observed.[3] We report here a more detailed study of this unique reaction.

Experimental Section

Materials. HEL and 5,7,12,14-tetraphenylpentacene (TP) were synthesized according to literature procedures.[4,5] The solvents used were spectroscopic grade purchased from Aldrich, except for carbon disulfide which was purchased from Merck (Uvasol series). All solvents were purified by column chromatography with neutral Al_2O_3 (Woelm). Tetramethylethylene (TME), 2,6-diphenylisobenzofuran (DPBF), and 2,6-di-*tert*-butyl-4-methylphenol were purchased from Aldrich and used without further purification.

Instruments. Spectroscopic measurements were performed on a Perkin-Elmer 555 or Lambda 5 UV-vis spectrometer. HPLC analyses were done with a Perkin-Elmer 3 B pump using a reversed-phase C_{18} column (Perkin-Elmer) (acetonitrile, Aldrich HPLC grade) and a spectrophotometric UV-vis detector (Perkin-Elmer LC-75) at 290 nm. ESR measurements were performed on a Varian E-12 spectrometer. In all experiments, the starting concentration of HEL was about 1×10^{-4} M, except for in acetonitrile, where its solubility is rather small (max. 5×10^{-5} M). Values for the oxygen concentration in the solvents used[6] are $[O_2] = 2 \times 10^{-3}$ M (air-saturated toluene), 9.5×10^{-3} M (oxygen-saturated toluene), 1.7×10^{-3} M (air-saturated acetonitrile), and 1.1×10^{-3} M (air-saturated iodobenzene).

Solutions with defined concentrations of O_2 were prepared by four pump-freeze-thaw cycles on a vacuum line at 10^{-3} mbar followed by addition of O_2.

In all measurements, extreme care was taken to protect the solutions from light exposure.

Results

1. Thermal Formation of HELPO. Air-saturated solutions of HEL ([HEL] = 8×10^{-5} M) in toluene were allowed to stand for 2 weeks in the dark at 298 K. After this time, the reaction mixture was analyzed with the following results.

1.1. HPLC Analysis. Only two compounds were detected in appreciable amounts (see Figure 2). They could be identified by their retention times as HEL (5.8 min) and HELPO (2.8 min).

(1) Acs, A.; Schmidt, R.; Brauer, H.-D. *Ber. Bunsenges. Phys. Chem.* **1987**, *91*, 1331-1337.
(2) Brauer, H.-D.; Acs, A.; Schmidt, R. *Ber. Bunsenges. Phys. Chem.* **1987**, *91*, 1337-1346.
(3) Aubry, J. H. *J. Am. Chem. Soc.* **1985**, *107*, 5844-5849.
(4) Clar, E. *Polycyclic Hydrocarbons*; Academic Press: London, 1964; Vol. 2, pp 47-50.
(5) Gabriel, R. Thesis, University of Frankfurt, Frankfurt/Main, FRG, 1987.
(6) Battino, R.; Rettich, T. R.; Tominaga, T. *J. Phys. Chem. Ref. Data* **1983**, *12*, 163-178.

0002-7863/92/1514-4486$03.00/0